Activation of H_2 over the Ru-Zn Bond in the Transition Metal-Lewis Acid Heterobimetallic Species $[Ru(IPr)_2(CO)ZnEt]^+$ (IPr = 1,3-bis(2,6-diisopropylphenyl)imidazol-2-ylidene)

Ian M. Riddlestone,[#] Nasir A. Rajabi,[§] John P. Lowe,[#] Mary F. Mahon,[#] Stuart A. Macgregor*,[§] and Michael K. Whittlesey*,[#]

[#] Department of Chemistry, University of Bath, Claverton Down, Bath BA2 7AY, UK

[§] Institute of Chemical Sciences, Heriot-Watt University, Edinburgh EH14 4AS, UK

Supporting Information Placeholder

ABSTRACT: Reaction of $[Ru(IPr)_2(CO)H]BAr^F_4$ with $ZnEt_2$ forms the heterobimetallic species $[Ru(IPr)_2(CO)ZnEt]BAr^F_4$ (**2**) which features an unsupported Ru-Zn bond. **2** reacts with H_2 to give $[Ru(IPr)_2(CO)(\eta^2\text{-}H_2)(H)_2ZnEt]BAr^F_4$ (**3**) and $[Ru(IPr)_2(CO)(H)_2ZnEt]BAr^F_4$ (**4**). DFT calculations indicate that H_2 activation at **2** proceeds via oxidative cleavage at Ru with concomitant hydride transfer to Zn. **2** can also activate hydridic E-H bonds (E = B, Si) and computed mechanisms for the facile H/H exchange processes observed in **3** and **4** are presented.

Metal-ligand cooperativity is a widely used strategy for the activation and catalytic transformation of small molecules.[1] Many such systems are predicated on transition metal-Lewis base (TM-LB) combinations,[2,3] as well as those featuring electronically flexible ligand scaffolds, exemplified by Milstein's (de)aromatization approach.[4] More recently, TM-LA (LA = Lewis acid) cooperativity has (re)emerged[5] with reports of H_2 cleavage,[6] the activation of C-H and more polar E-H bonds[6a,6f,7] and, in some cases, involvement in catalytic processes.[6a,6b,7,8] To date such TM-LA cooperativity has been dominated by cases where the LA is a B or Al center that is brought into proximity with the TM via a constrained geometry ligand, typically a bi- or polydentate P- or N-based species.[6-9] Herein, we report on the preparation and reactivity of a novel TM-LA system, $[Ru(IPr)_2(CO)ZnEt]BAr^F_4$ (**2**)[10] which features a direct, unsupported Ru-Zn bond and is accessed via the simple addition of $ZnEt_2$ to $[Ru(IPr)_2(CO)H]BAr^F_4$ (**1**).[11] Complex **2** can activate H_2 with net addition across the Ru-Zn bond to give $[Ru(IPr)_2(CO)(\eta^2\text{-}H_2)(H)_2ZnEt]BAr^F_4$ (**3**).[12] The observation of facile intramolecular H/H exchange in **3**, along with DFT calculations, highlight the ability of the TM-LA {RuZn} moiety to act as a flexible and reversible hydride shuttle.

In line with the reported electrophilic reactivity of the hydride ligand in $[Ru(IPr)_2(CO)H]BAr^F_4$ (**1**),[11] addition of one equivalent of $ZnEt_2$ to a fluorobenzene solution of this species gave the Ru-Zn complex **2** (Scheme 1), which was isolated as a red solid in 76% yield. ^{1}H NMR spectroscopy confirmed the absence of any hydride ligand in **2** and confirmed the presence of a single ZnEt group on the basis of the 8:3:2 ratio of ^{i}Pr methine protons to low frequency signals at δ 0.73 (CH_3) and δ -0.11 (CH_2).

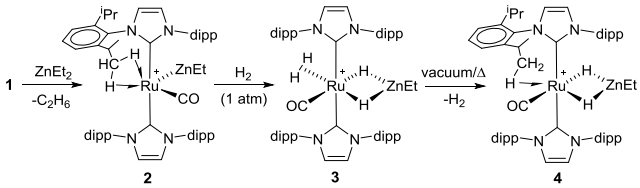

Scheme 1. Formation and reactivity of **2**-**4** (dipp = 2,6-diisopropylphenyl). BAr^F_4 anions not shown.

Upon shaking a C_6H_5F solution of **2** under H_2 (1 atm), there was an instantaneous color change (deep red to colorless) resulting from the formation of the novel dihydrogen dihydride complex $[Ru(IPr)_2(CO)(\eta^2\text{-}H_2)(H)_2ZnEt]BAr^F_4$ (**3**, Scheme 1). The ^{1}H NMR spectrum of **3** exhibited two hydride resonances, a broad signal at δ -5.33 and a sharp peak at δ -12.13, in a relative ratio of 3:1. Cooling to -28 °C resolved the broad resonance into two signals (relative ratio 2:1) at δ -5.09 and -7.79 (with T_1 values of 31 and 72 ms respectively)[13] assigned to $Ru(\eta^2\text{-}H_2)$ and Ru-H-Zn (trans to CO) respectively. Both signals remained broad, indicative of exchange; this was confirmed by EXSY and magnetization transfer experiments (Figure S11). No exchange with the remaining Ru-H-Zn trans to dihydrogen (δ -12.13, T_1 = 809 ms; T_1(min) = 638 ms (CD_2Cl_2, 400 MHz, -41 °C)) was found. However, upon exposure of **3** to 1 atm D_2, ^{1}H and ^{2}H NMR spectra showed unequivocally that all three sites underwent a slower chemical exchange with deuterium incorporated into the $Ru(\eta^2\text{-}H_2)$ and at both Ru-H-Zn positions.

The $\eta^2\text{-}H_2$ ligand in **3** proved hard to dissociate, with only ca. 20% conversion to $[Ru(IPr)_2(CO)(H)_2ZnEt]BAr^F_4$ (**4**) apparent even after evaporating a C_6H_5F solution of **3** to complete dryness. In fact, full conversion to **4** required heating a solid sample of **3** at 50 °C under dynamic vacuum for 24 h. Subjecting solid **3** to vacuum/heat for further time (ca. 72 h) showed that all four hydride ligands could be removed, although reformation of **2** was also accompanied by additional, unidentified side products. Complex **4** displayed a low frequency (δ -27.06) Ru-H-Zn signal which now exchanged on the NMR timescale (magnetization transfer and EXSY measurements; Figure S12) with a second Ru-H-Zn resonance at δ -3.75.

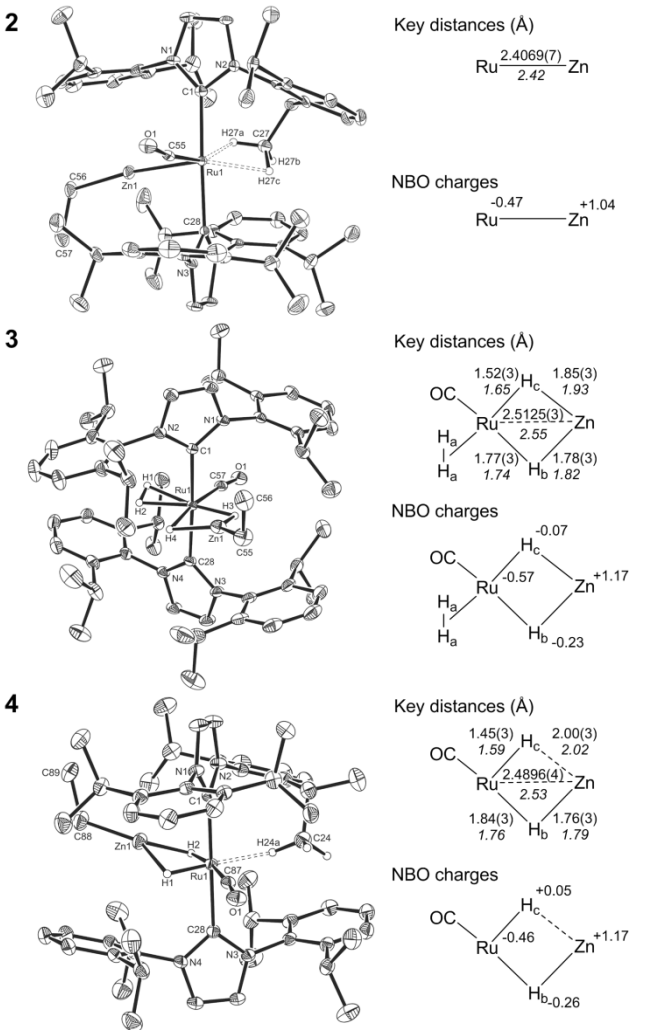

Figure 1. Molecular structures of the cations in **2**, **3** and **4**. Thermal ellipsoids are shown at 30%. All non-hydride and non-agostic hydrogen atoms are omitted for clarity. Also shown are comparisons of the key experimental and (in italics) computed distances around the central {Ru-Zn} moiety, along with the accompanying NBO charges.

The molecular structures of the cations in **2**, **3** and **4** are shown in Figure 1, along with a comparison with computed data for the central $\{Ru(H)_nZn\}$ moieties in each case (n = 0, 4 and 2 respectively). **2** exhibits a Ru-Zn distance of 2.4069(7) Å,[14] and also features two short Ru···H-C agostic interactions to one of the IPr ligands (Ru(1)···H(27A)-C(27) 2.13(3) Å, Ru(1)···H(27C)-C(27) 2.31(4) Å), similar to those seen previously in **1**.[11] In **3** and **4** the η^2-H_2 and hydride hydrogens were included in the model, the latter being refined without restraint. Both these species have elongated Ru-Zn distances (2.5125(3) Å and 2.4896(4) Å, respectively) and have distinctly asymmetric $\{Ru(H)_2Zn\}$ moieties that reflect the relative trans influences of the ligands completing the coordination sphere. Thus, the bridging hydrides trans to CO in **3** and **4** are approximately evenly shared between Ru and Zn, whereas the hydride trans to η^2-H_2 in **3** is significantly closer to Ru. This asymmetry is even more marked for the hydride trans to the agostic interaction in **4**.

DFT calculations[15] provide good absolute agreement for both the Ru-Zn distances as well as the various Ru-H and Zn-H distances in **2**, **3** and **4**, allowing for the inherent uncertainty in the H atom positions (see Figure 1, right hand side). NBO calculations characterize **2** as a Ru(0) species interacting with a cationic $\{ZnEt\}^+$ moiety via Ru →Zn σ-donation. In contrast, no significant direct Ru-Zn interaction is seen in either **3** or **4** (see Supporting Information for full details and orbital plots). NPA charges were used to characterize the nature of the hydride ligands. These indicate that the more evenly shared hydrides, H_b (trans to CO in **3** and **4**), exhibit a significant negative charge (q_H = -0.23 and -0.26 respectively) while this reduces and becomes positive as the hydride moves closer to Ru (H_c: q_H = -0.07 trans to η^2-H_2 in **3**; q_H = +0.05 trans to the agostic in **4**). For comparison the terminal hydride in **1** (which lies trans to a vacant site) has q_H = +0.16. H_c in **4** therefore more resembles a terminal Ru-hydride: indeed an Atoms in Molecules study on **4** shows the absence of any Zn···H_c bond path (Figure S14).[16] The $\{Ru(H)_2Zn\}$ moieties in these species are therefore structurally flexible and able to access both bridging and terminal hydride character depending on the precise coordination environment.

Although examples of $\{M(H)_nZn\}$ complexes exist for M = Ru,[17] as well as for other late TMs,[18] these all result from metal hydride precursors and, to the best of our knowledge, formation via bimetallic M-Zn cleavage of H_2 has no precedent.[19,20] We have therefore used DFT calculations to study the formation of **2** as well as its onwards reactivity with H_2 to **3** and **4**. Figure 2 indicates that the initial addition of $ZnEt_2$ to **1** forms an intermediate **I(1-2)1** at -12.3 kcal/mol in which the {RuZn} moiety is bridged by both a hydride and an ethyl ligand; the latter also engages in a β-agostic interaction with the Ru center. Ethyl group transfer onto Ru proceeds via **TS(1-2)1** with a barrier of 11.1 kcal/mol and is induced by rotation of the {Ru(H)Zn} moiety such that the bridging hydride drops below the equatorial coordination plane. This allows the CO ligand to move trans to the developing Ru-Et ligand (**I(1-2)2**, G = -13.7 kcal/mol). The bridging hydride can now couple with the adjacent ethyl group via **TS(1-2)2** at -6.9 kcal/mol leading, after release of ethane, to the formation of **2** at -30.4 kcal/mol. In this case an alternative isomer of **2** devoid of agostic interactions is located, similar to the situation described previously for **1** for which several isomers were also found.[11]

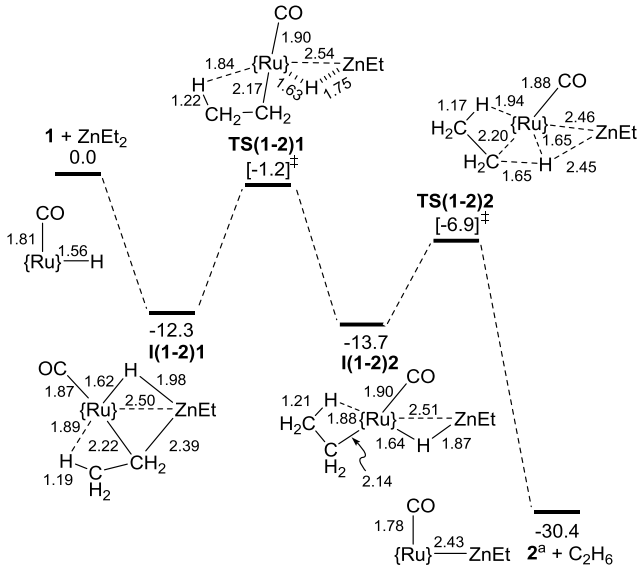

Figure 2. Computed reaction profile (free energy, kcal/mol) for the formation of **2** and C_2H_6 from **1** and $ZnEt_2$; schematic structures show key distances (Å) within the equatorial plane; {Ru} = $Ru(IPr)_2^+$. An ethane σ-complex, **I(1-2)3**, generated from **TS(1-2)2** is omitted for clarity. [a] non-agostic isomer of **2** located.

Figure 3 shows one possible mechanism for the reaction of **2** with H_2 to give **3** and **4**. Addition of two molecules of H_2 to **2** forms the bis-η^2-H_2 intermediate **I(2-3)1** at -32.1 kcal/mol. A very flat free energy surface then sees an essentially barrierless cleavage of the H_b-H_c ligand with net addition over the Ru-Zn bond to give **I(2-3)2** at -34.8 kcal/mol. Rotation about the Ru···Zn vector then allows transfer of H_b onto Zn to form **3** at -41.4 kcal/mol. H_2 loss from **3** is computed to be kinetically accessible ($\Delta G^{\ddagger}$ = 15.8 kcal/mol), but endergonic, **4** (+ H_2) lying 5 kcal/mol above **3**. This is consistent with the reluctance of this species to lose H_2 found experimentally.

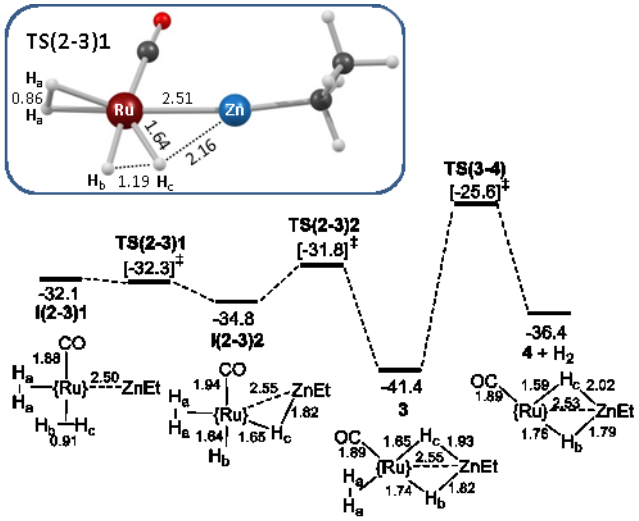

Figure 3. Computed reaction profile (free energy, kcal/mol) for the formation of **3** and **4** from **2**; schematic structures show key distances (Å) in the equatorial plane, as well as the labelling scheme for the H atoms; {Ru} = $Ru(IPr)_2^+$. Inset: geometry of H_2 activation transition state **TS(2-3)1** (IPr ligands omitted).

The computed structure of the key H_2 activation transition state **TS(2-3)1** (inset, Figure 3) exhibits an elongated H_b-H_c moiety (1.19 A *cf.* 0.91 A in **I(2-3)1**). At this point the Zn···H_c distance of 2.16 A implies little, if any, interaction with the Zn center and it is only after the cleavage that the Zn participates by accepting a hydride ligand. In addition, minimal polarization of the H_b-H_c bond is computed in the transition state (q_{Hb} = +0.05; q_{Hc} = +0.02). We therefore propose that H_2 activation occurs via oxidative cleavage mediated by Ru, followed by hydride transfer to Zn. In support of Ru being the key player in the H_2 cleavage, the activation of H_a-H_a trans to Zn in **I(2-3)1** was also characterized: this proceeds via a structurally similar transition state at -28.6 kcal/mol which leads to a Ru(η^2-H_2)(H_2) complex in which the Zn is unable accept either hydride (Figure S17).

The mechanisms of H/H exchange in **3** and **4** have also been modelled. For **3**, exchange occurs both between the η^2-H_2 ligand and the cis bridging hydride (H_a/H_b exchange) as well as between the two chemically distinct bridging hydrides (H_b/H_c exchange). H_b/H_c exchange can proceed via the mechanism in Figure 3, with reversible formation of the bis-η^2-H_2 complex **I(2-3)1** and rotation of the H_b-H_c ligand. The latter occurs via a transition state at -28.3 kcal/mol, giving an overall exchange barrier of 13.1 kcal/mol. For H_a/H_b exchange a σ-CAM process[21] was characterized that sees formation of the H_a/(η^2-H_a-H_b) complex, **I(3-3')** (Figure 4a). H_a-H_b rotation and reversing the σ-CAM completes the exchange, the rotation transition state being the highest point in this process and equating to an overall barrier of 9.8 kcal/mol. The lower barrier for H_a/H_b exchange is consistent with the EXSY experiments that indicated that only that process proceeded on the NMR timescale.[22] H_b/H_c exchange in **4** proceeds by a similar mechanism to that in **3** (Figure 4b). Thus initial rotation about the Ru···Zn vector cleaves the Zn-H_b bond and forms **I(4-4')1**; H_c can then transfer onto H_b to form the η^2-H_b-H_c complex **I(4-4')2**. H_2 rotation and reversing these processes complete the exchange. The highest transition states in this process are at -22.9 kcal/mol and correspond to an overall barrier of 13.5 kcal/mol. In principle, movement of the CO ligand from trans to H_b to trans to H_c would also render these two sites equivalent. However, this process has a barrier of 31.5 kcal/mol as it passes through a symmetrical Y-shaped {$RuCO(H)_2$} moiety, which is strongly disfavored for a d^6 configuration.[23]

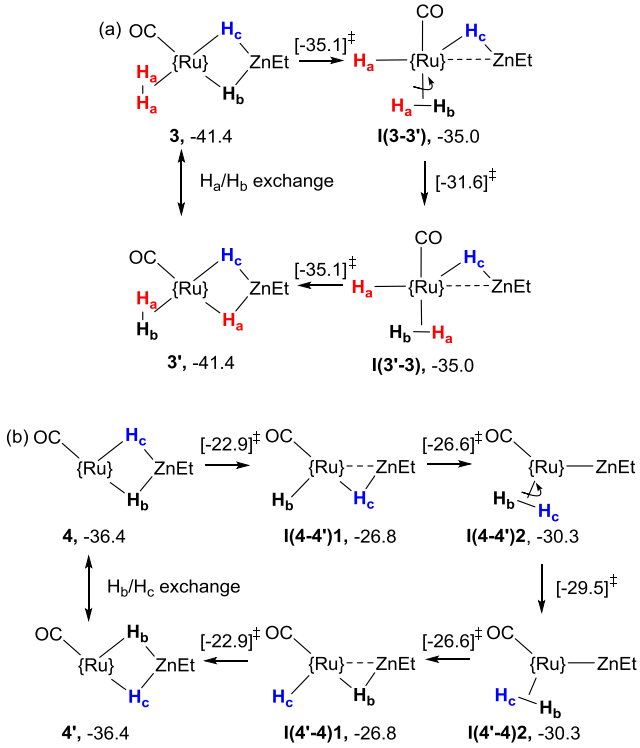

Figure 4. Computed mechanisms (free energy, kcal/mol) for (a) H_a/H_b in **3** and (b) H_b/H_c in **4**; {Ru} = $Ru(IPr)_2^+$. Transition state energies for each step are given in square brackets.

To probe whether other E-H bonds could add across the Ru-Zn bond in **2**, preliminary investigations with both protic and hydridic reagents have been undertaken. NH_3 simply coordinated to form the ammonia complex $[Ru(IPr)_2(CO)(NH_3)ZnEt]BAr^F{}_4$ (**5**; Figure S13). With HBcat and $PhSiH_3$, room temperature dehydrogenation took place to give **3** as the major ruthenium-containing product of both reactions. Surprisingly, even a 1:1 ratio of **2**:HBcat generated hydride signals characteristic of **3** suggesting that a strong driving force exists for formation of the $Ru(H)_2Zn$ moiety. ^{11}B NMR spectroscopy confirmed the formation of B_2cat_2 (δ 31), but also showed a second major product at δ 22 which, by comparison to the literature, appears to be B_2cat_3.[25] In the reaction of **2** with $PhSiH_3$, ^{29}Si NMR spectroscopy showed that Ph_3SiH and Ph_2SiH_2 were the major silicon containing reaction products, although a number of other, lower intensity signals were also present which we believe arise from the presence of three reactive Si-H bonds in the starting material, as well as the need for SiH_4 formation for atom balance. There is a clear silane dependence to this chemistry since no reaction was seen between **2** and either

Ph_2SiH_2 or $PhMe_2SiH$. Further studies are required to elucidate the pathways of the borane/silane dehydrogenation reactions.

In conclusion, we have described the facile formation of the TM-LA heterobimetallic species, **2**, featuring an unconstrained and unsupported Ru-Zn bond. This species is a rare example of an active TM-LA system derived from a non-group 13 element LA: **2** reacts directly with H_2 to form the $\{Ru(H)_2Zn\}$ species **3** and then **4**. DFT calculations indicate that H_2 activation proceeds via oxidative cleavage at Ru with the adjacent Zn acting as a (reversible) hydride acceptor. H/H exchange experiments and calculations on **3** and **4** show that intermediates with unsupported Ru-Zn bonds remain kinetic accessibility even after H_2 addition. This, along with the observation of the activation of hydridic E-H bonds (E = B, Si), suggests that such unconstrained heterobimetallic TM-LA species may have potential applications in catalysis and this possibility is being pursued in our laboratories.

ASSOCIATED CONTENT

Supporting Information

All data supporting this study are provided as Supporting Information accompanying this paper. This includes: synthesis, characterization (inc. multinuclear NMR spectra) and crystallographic data (CIF) for **2-5**; computational data, including computed geometries and energies, details of alternative reaction pathways and a molecular graph of **4**. This material is available free of charge via the Internet at http://pubs.acs.org.

AUTHOR INFORMATION

Corresponding Authors

s.a.macgregor@hw.ac.uk; m.k.whittlesey@bath.ac.uk

Notes

The authors declare no competing financial interests.

ACKNOWLEDGMENT

We acknowledge financial support from the EPSRC (grant EP/J009962/1 for IMR) and Heriot-Watt University (James Watt Scholarship to NAR). We would like to thank Professor Ged Parkin for enlightening and very valuable discussions.

REFERENCES

(1) (a) Cooper, B. G.; Napoline, J. W.; Thomas, C. M. *Catal. Rev.: Sci. Eng.* **2011**, *54*, 1. (b) van der Vlugt, J. I. *Eur. J. Inorg. Chem.* **2012**, 363. (c) Eisenstein, O.; Crabtree, R. H. *New. J. Chem.* **2013**, *37*, 21. (d) Khusnutdinova, J. R.; Milstein, D. *Angew. Chem. Int. Ed.* **2015**, *54*, 12236. (e) Bouhadir, G.; Bourissou, D. *Chem. Soc. Rev.* **2015**, *45*, 1065.

(2) For LB = N, see: (a) Noyori, R.; Ohkuma, T. *Angew. Chem. Int. Ed. Engl.* **2001**, *40*, 40. (b) Sandoval, C. A.; Ohkuma, T.; Muñiz, K.; Noyori, R. *J. Am. Chem. Soc.* **2003**, *125*, 13490. (c) Maire, P.; Büttner, T.; Breher, F.; Le Floch, P.; Grützmacher, H. *Angew. Chem. Int. Ed.* **2005**, *44*, 6318. (d) Friedrich, A.; Drees, M.; Schmedt auf der Günne, J.; Schneider, S. *J. Am. Chem. Soc.* **2009**, *131*, 17552.

(3) For LB = O or S, see: (a) Sweeney, Z. K.; Polse, J. L.; Bergman, R. G.; Andersen, R. A. *Organometallics* **1999**, *18*, 5502. (b) Linck, R. C.; Pafford, R. J.; Rauchfuss, T. B. *J. Am. Chem. Soc.* **2001**, *123*, 8856. (c) Sellmann, D.; Prakash, R.; Heinemann, F. W.; Moll, M.; Klimowicz, M. *Angew. Chem. Int. Ed.* **2004**, *43*, 1877. (d) Ohki, Y.; Sakamoto, M.; Tatsumi, K. *J. Am. Chem. Soc.* **2008**, *130*, 11610. (e) Matsumoto, T.; Nakaya, Y.; Itakura, N.; Tatsumi, K. *J. Am. Chem. Soc.* **2008**, *130*, 2458. (f) Klare, H. F. T.; Oestreich, M.; Ito, J.; Nishiyama, H.; Ohki, Y.; Tatsumi, K. *J. Am. Chem. Soc.* **2011**, *133*, 3312.

(4) Gunanathan, C.; Milstein, D. *Acc. Chem. Res.* **2011**, *44*, 588.

(5) For early work on TM-LA complexes, see: (a) St. Denis, J. N.; Butler, W.; Glick, M. D.; Oliver, J. P. *J. Organomet. Chem.* **1977**, *129*, 1. (b) Burlitch, J. M.; Leonowicz, M. E.; Petersen, R. B.; Hughes, R. E. *Inorg. Chem.* **1979**, *18*, 1097. For recent, pertinent reviews, see: (c) Amgoune, A.; Bourissou, D. *Chem. Commun.* **2011**, *47*, 859. (d) Maity, A.; Teets, T. S. *Chem. Rev.* **2016**, DOI: 10.1021/acs.chemrev.6b00034.

(6) (a) Harman, W. H.; Peters, J. C. *J. Am. Chem. Soc.* **2012**, *134*, 5080. (b) Lin, T.P.; Peters, J. C. *J. Am. Chem. Soc.* **2013**, *135*, 15310. (c) Zeng, G.; Sakaki, S. *Inorg. Chem.* **2013**, *52*, 2844. (d) Harman, W. H.; Lin, T.-P.; Peters, J. C. *Angew. Chem. Int. Ed.* **2014**, *53*, 1081. (e) Cowie, B. E.; Emslie, D. J. H. *Chem. Eur. J.* **2014**, *20*, 16899. (f) Barnett, B. R.; Moore, C. E.; Rheingold, A. L.; Figueroa, J. S. *J. Am. Chem. Soc.* **2014**, *136*, 10262. (g) Devillard, M.; Bouhadir, G.; Bourissou, D. *Angew. Chem. Int. Ed.* **2015**, *54*, 730. (h) Li, Y.; Hou, C.; Jiang, J.; Zhang, Z.; Zhao, C.; Page, A. J.; Ke, Z. *ACS Catal.* **2016**, *6*, 1655. (i) Devillard, M.; Declercq, R.; Nicolas, E.; Ehlers, A. W.; Backs, J.; Saffon-Merceron, N.; Bouhadir, G.; Slootweg, J. C.; Uhl, W.; Bourissou, D. *J. Am. Chem. Soc.* **2016**, *138*, 4917.

(7) (a) Fong, H.; Moret, M.-E.; Lee, Y.; Peters, J. C. *Organometallics* **2013**, *32*, 3053. (b) MacMillan, S. N.; Harman, W. H.; Peters, J. C. *Chem. Sci.* **2014**, *5*, 590. (c) Nesbit, M. A.; Suess, D. L. M.; Peters, J. C. *Organometallics* **2015**, *34*, 4741.

(8) (a) Tsoureas, N.; Kuo, Y.-Y.; Haddow, M. F.; Owen, G. R. *Chem. Commun.* **2011**, *47*, 484. (b) Cammarota, R. C.; Lu, C. C. *J. Am. Chem. Soc.* **2015**, *137*, 12486.

(9) (a) Bontemps, S.; Bouhadir, G.; W., G.; Mercy, M.; Chen, C.-H.; Foxman, B. M.; Maron, L.; Ozerov, O. V.; Bourissou, D. *Angew. Chem. Int. Ed.* **2008**, *47*, 1481. (b) Sircoglou, M.; Bontemps, S.; Bouhadir, G.; Saffon, N.; Miqueu, K.; Gu, W.; Mercy, M.; Chen, C.-H.; Foxman, B. M.; Maron, L.; Ozerov, O. V.; Bourissou, D. *J. Am. Chem. Soc.* **2008**, *130*, 16729. (c) Rudd, P. A.; Liu, S.; Gagliardi, L.; Young, V. G.; Lu, C. C. *J. Am. Chem. Soc.* **2011**, *133*, 20724. (d) Cowie, B. E.; Tsao, F. A.; Emslie, D. J. H. *Angew. Chem. Int. Ed.* **2015**, *54*, 2165.

(10) IPr = 1,3-bis(2,6-diisopropylphenyl)imidazol-2-ylidene; BAr_4^F = $B\{C_6H_3(3,5\text{-}CF_3)_2\}_4^-$.

(11) Riddlestone, I. M.; McKay, D.; Gutmann, M. J.; Macgregor, S. A.; Mahon, M. F.; Sparkes, H. A.; Whittlesey, M. K. *Organometallics* **2016**, *35*, 1301.

(12) For a recent review of molecular Zn-H complexes, see: Wiegand, A.-K.; Rit, A.; Okuda, J. *Coord. Chem. Rev.* **2016**, *314*, 71.

(13) In CD_2Cl_2, a T_1 value of 47 ms was measured for the Ru-H-Zn resonance at δ -7.79 at -28 °C. The value increased upon cooling: 93 ms at -41 °C, 205 ms at -55 °C and 323 ms at -68 °C.

(14) (a) Cadenbach, T.; Bollermann, T.; Gemel, C.; Tombul, M.; Fernandez, I.; von Hopffgarten, M.; Frenking, G.; Fischer, R. A. *J. Am. Chem. Soc.* **2009**, *131*, 16063. (b) Bollermann, T.; Gemel, C.; Fischer, R. A. *Coord. Chem. Rev.* **2012**, *256*, 537.

(15) Calculations were run with the Gaussian suite of programs and employed the BP86 functional. Free energies include corrections for fluorobenzene solvent and dispersion effects. See Supporting Information for references and full details.

(16) As a result of the ambiguity regarding the nature of the hydrides in the $\{Ru(H)_2Zn\}$ moiety, the half-arrow formalism (Green, J. C.; Green, M. L. H.; Parkin, G. *Chem. Commun.* **2012**, *48*, 11481) has not been adopted.

(17) (a) Ohashi, M.; Matsubara, K.; Iizuka, T.; Suzuki, H. *Angew. Chem. Int. Ed.* **2003**, *42*, 937. (b) Ohashi, M.; Matsubara, K.; Suzuki, H. *Organometallics* **2007**, *26*, 2330. (c) Plois, M.; Hujo, W.; Grimme, S.; Schwickert, C.; Bill, E.; de Bruin, B.; Pöttgen, R.; Wolf, R. *Angew. Chem. Int. Ed.* **2013**, *52*, 1314. (d) Molon, M.; Gemel, C.; Fischer, R. A. *Eur. J. Inorg. Chem.* **2013**, 3616. (e) Plois, M.; Wolf, R.; Hujo, W.; Grimme, S. *Eur. J. Inorg. Chem.* **2013**, 3039.

(18) (a) Geerts, R. L.; Huffman, J. C.; Caulton, K. G. *Inorg. Chem.* **1986**, *25*, 590. (b) Fryzuk, M. D.; McConville, D. H.; Rettig, S. J. *Organometallics* **1993**, *12*, 2152. (c) Ekkert, O.; White, A. J. P.; Toms, H.; Crimmin, M. R. *Chem. Sci.* **2015**, *6*, 5617.

(19) For examples of Zn-H bond formation by activation of H_2, see: (a) Jochmann, P.; Stephan, D. W. *Angew. Chem. Int. Ed.* **2013**, *52*, 9831. (b) Jochmann, P.; Stephan, D. W. *Chem. Commun.* **2014**, *50*, 8395.

(20) Fafard, C. M.; Chen, C.-H.; Foxman, B. M.; Ozerov, O. V. *Chem. Commun.* **2007**, 4465.

(21) Perutz, R. N.; Sabo-Etienne, S. *Angew. Chem. Int. Ed.* **2007**, *46*, 2578.

(22) An pathway linking **I(2-3)2** (Figure 3) to **I(3-3')** (Figure 4a) was also characterized and provides an alternative route from **2** to **3** via a transition state at -31.2 kcal/mol (see Figure S18).

(23) Riehl, J.-F.; Jean, Y.; Eisenstein, O.; Pélissier, M. *Organometallics* **1992**, *11*, 729.

(24) Westcott, S. A.; Blom, H. P.; Marder, T. B.; Baker, R. T.; Calabrese, J. C. *Inorg. Chem.* **1993**, *32*, 2175.

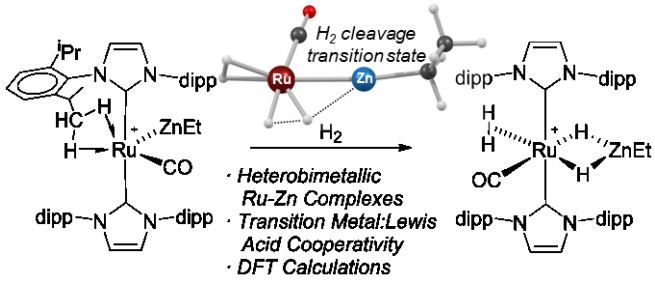
iPr
dipp
HC
H
Ru
ZnEt
CO
dipp
dipp
H_2 cleavage transition state
Ru
Zn
H_2
dipp
dipp
H
H
Ru
H
ZnEt
OC
H
dipp
dipp
· Heterobimetallic Ru-Zn Complexes
· Transition Metal:Lewis Acid Cooperativity
· DFT Calculations